Recording oscillations of sub-micron size cantilevers by extreme ultraviolet Fourier transform holography

Nils C. Monserud,[1] Erik B. Malm,[1] Przemyslaw W. Wachulak,[2] Vakhtang Putkaradze,[3] Ganesh Balakrishnan,[4] Weilun Chao,[5] Erik Anderson,[5] David Carlton,[5] and Mario C. Marconi[1,*]

[1]*Engineering Research Center for Extreme Ultraviolet Science and Technology, and Electrical and Computer Engineering Department, Colorado State University, Fort Collins, Colorado 80523, USA*
[2]*Institute of Optoelectronics, Military University of Technology, ul. gen. S. Kaliskiego 2, 00-908 Warsaw, Poland*
[3]*Department of Mathematics and Statistical Sciences, University of Alberta, T6G 2R3 Canada*
[4]*Center for High Technology Materials, and Department of Electrical and Computer Engineering, University of New Mexico, Albuquerque, New Mexico 87106, USA*
[5]*Center for X-Ray Optics, Lawrence Berkeley National Lab, 1 Cyclotron Rd, Berkeley, California 94720, USA*

Abstract: We recorded the fast oscillation of sub-micron cantilevers using time-resolved extreme ultraviolet (EUV) Fourier transform holography. A tabletop capillary discharge EUV laser with a wavelength of 46.9 nm provided a large flux of coherent illumination that was split using a Fresnel zone plate to generate the object and the reference beams. The reference wave was produced by the first order focus while a central opening in the zone plate provided a direct illumination of the cantilevers. Single-shot holograms allowed for the composition of a movie featuring the fast oscillation. Three-dimensional displacements of the object were determined as well by numerical back-propagation, or "refocusing" of the electromagnetic fields during the reconstruction of a single hologram.

References and links

1. C. A. Brewer, F. Brizuela, P. Wachulak, D. H. Martz, W. Chao, E. H. Anderson, D. T. Attwood, A. V. Vinogradov, I. A. Artyukov, A. G. Ponomareko, V. V. Kondratenko, M. C. Marconi, J. J. Rocca, and C. S. Menoni, "Single-shot extreme ultraviolet laser imaging of nanostructures with wavelength resolution," Opt. Lett. **33**(5), 518–520 (2008).
2. S. Carbajo, I. D. Howlett, F. Brizuela, K. S. Buchanan, M. C. Marconi, W. Chao, E. H. Anderson, I. Artioukov, A. Vinogradov, J. J. Rocca, and C. S. Menoni, "Sequential single-shot imaging of nanoscale dynamic interactions with a table-top soft x-ray laser," Opt. Lett. **37**(14), 2994–2996 (2012).
3. P. W. Wachulak, M. C. Marconi, R. A. Bartels, C. S. Menoni, and J. J. Rocca, "Soft x-ray laser holography with wavelength resolution," J. Opt. Soc. Am. B **25**(11), 1811–1814 (2008).
4. P. W. Wachulak, M. C. Marconi, R. A. Bartels, C. S. Menoni, and J. J. Rocca, "Volume extreme ultraviolet nano-holographic imaging with numerical optical sectioning," Opt. Express **15**(17), 10622–10628 (2007).
5. M. M. Murnane and J. W. Miao, "OPTICS: Ultrafast X-ray photography," Nature **460**(7259), 1088–1090 (2009).
6. R. L. Sandberg, A. Paul, D. A. Raymondson, S. Hädrich, D. M. Gaudiosi, J. Holtsnider, R. I. Tobey, O. Cohen, M. M. Murnane, H. C. Kapteyn, C. G. Song, J. W. Miao, Y. W. Liu, and F. Salmassi, "Lensless diffractive imaging using tabletop coherent high-harmonic soft-x-ray beams," Phys. Rev. Lett. **99**(9), 098103 (2007).
7. R. L. Sandberg, D. A. Raymondson, C. La-O-Vorakiat, A. Paul, K. S. Raines, J. Miao, M. M. Murnane, H. C. Kapteyn, and W. F. Schlotter, "Tabletop soft-x-ray Fourier transform holography with 50 nm resolution," Opt. Lett. **34**(11), 1618–1620 (2009).
8. P. Thibault, V. Elser, C. Jacobsen, D. Shapiro, and D. Sayre, "Reconstruction of a yeast cell from X-ray diffraction data," Acta Crystallogr. A **62**(4), 248–261 (2006).
9. E. Guehrs, A. M. Stadler, S. Flewett, S. Frommel, J. Geilhufe, B. Pfau, T. Rander, S. Schaffert, G. Buldt, and S. Eisebitt, "Soft x-ray tomoholography," New J. Phys. **14**(1), 013022 (2012).

10. J. W. Miao, C. C. Chen, C. Y. Song, Y. Nishino, Y. Kohmura, T. Ishikawa, D. Ramunno-Johnson, T. K. Lee, and S. H. Risbud, "Three-dimensional GaN-Ga2O3 core shell structure revealed by X-ray diffraction microscopy," Phys. Rev. Lett. **97**(21), 215503 (2006).
11. I. Peterson, B. Abbey, C. T. Putkunz, D. J. Vine, G. A. van Riessen, G. A. Cadenazzi, E. Balaur, R. Ryan, H. M. Quiney, I. McNulty, A. G. Peele, and K. A. Nugent, "Nanoscale Fresnel coherent diffraction imaging tomography using ptychography," Opt. Express **20**(22), 24678–24685 (2012).
12. K. S. Raines, S. Salha, R. L. Sandberg, H. D. Jiang, J. A. Rodríguez, B. P. Fahimian, H. C. Kapteyn, J. C. Du, and J. W. Miao, "Three-dimensional structure determination from a single view," Nature **463**(7278), 214–217 (2010).
13. C. M. Günther, B. Pfau, R. Mitzner, B. Siemer, S. Roling, H. Zacharias, O. Kutz, I. Rudolph, D. Schondelmaier, R. Treusch, and S. Eisebitt, "Sequential femtosecond X-ray imaging," Nat. Photonics **5**(2), 99–102 (2011).
14. B. Pfau, C. M. Gunther, S. Schaffert, R. Mitzner, B. Siemer, S. Roling, H. Zacharias, O. Kutz, I. Rudolph, R. Treusch, and S. Eisebitt, "Femtosecond pulse x-ray imaging with a large field of view," New J. Phys. **12**(9), 095006 (2010).
15. M. Guizar-Sicairos and J. R. Fienup, "Holography with extended reference by autocorrelation linear differential operation," Opt. Express **15**(26), 17592–17612 (2007).
16. S. G. Podorov, K. M. Pavlov, and D. M. Paganin, "A non-iterative reconstruction method for direct and unambiguous coherent diffractive imaging," Opt. Express **15**(16), 9954–9962 (2007).
17. I. McNulty, J. Kirz, C. Jacobsen, E. H. Anderson, M. R. Howells, and D. P. Kern, "High-Resolution Imaging by Fourier Transform X-Ray Holography," Science **256**(5059), 1009–1012 (1992).
18. E. B. Malm, N. C. Monserud, C. G. Brown, P. W. Wachulak, H. W. Xu, G. Balakrishnan, W. L. Chao, E. Anderson, and M. C. Marconi, "Tabletop single-shot extreme ultraviolet Fourier transform holography of an extended object," Opt. Express **21**(8), 9959–9966 (2013).
19. J. W. Goodman, *Introduction to Fourier Optics* (Roberts and Company, 2005).
20. C. D. Macchietto, B. R. Benware, and J. J. Rocca, "Generation of millijoule-level soft-x-ray laser pulses at a 4-Hz repetition rate in a highly saturated tabletop capillary discharge amplifier," Opt. Lett. **24**(16), 1115–1117 (1999).
21. L. Urbanski, M. C. Marconi, L. M. Meng, M. Berrill, O. Guilbaud, A. Klisnick, and J. J. Rocca, "Spectral linewidth of a Ne-like Ar capillary discharge soft-x-ray laser and its dependence on amplification beyond gain saturation," Phys. Rev. A **85**(3), 033837 (2012).
22. Y. Liu, M. Seminario, F. G. Tomasel, C. Chang, J. J. Rocca, and D. T. Attwood, "Achievement of essentially full spatial coherence in a high-average-power soft-x-ray laser," Phys. Rev. A **63**(3), 033802 (2001).
23. D. Brake, H. W. Xu, A. Hollowell, G. Balakrishnan, C. Hains, M. Marconi, and V. Putkaradze, "Intrinsic localized modes in two-dimensional vibrations of crystalline pillars and their application for sensing," J. Appl. Phys. **112**(10), 104326 (2012).
24. D. Brake and V. Putkaradze, "Simplified models for Intrinsic Localized Mode dynamics," in Proceedings of 2012 International Symposium on Nonlinear Theory and its Applications (2012)
25. A. J. Sievers and S. Takeno, "Intrinsic Localized Modes in Anharmonic Crystals," Phys. Rev. Lett. **61**(8), 970–973 (1988).
26. M. Sato, B. E. Hubbard, and A. J. Sievers, "Colloquium: Nonlinear energy localization and its manipulation in micromechanical oscillator arrays," Rev. Mod. Phys. **78**(1), 137–157 (2006).

1. Introduction

The fast evolution of nanoscale technologies requires new diagnostic techniques and imaging methods capable to achieve time-resolved spatial resolution at the nanoscale level. One possible methodology to improve the resolution on the imaging system is to utilize short wavelengths in the extreme ultraviolet (EUV) and soft X-ray region of the spectrum. Full field microscopy in the EUV has reached spatial resolutions comparable to the wavelength and the capability of acquiring time resolved images, however the image is restricted to one plane [1, 2]. EUV Gabor holograms recorded in the surface of a photoresist and subsequently numerically reconstructed reached spatial resolution of sub-50 nm comparable to the wavelength [3]. Further numerical processing of the reconstruction allowed for retrieving 3-D information [4]. However, this method requires processing of the hologram after-exposure and is intrinsically incapable of time-resolved images of the object. The improved spatial resolution of imaging techniques when utilizing EUV photons also introduces extra experimental complications in the implementation of the setup due to the limited availability of high efficiency optics. This is the reason why there are a handful of imaging techniques where the utilization of EUV light still constitutes a real advantage. At EUV and soft X-ray wavelengths, two leading imaging techniques are Fourier transform holography (FTH) and coherent diffraction imaging (CDI) employing iterative phase retrieval (IPR) [5–7]. Both

techniques are attractive as they provide a powerful method to image nanoscale objects with high spatial resolution, simultaneously retrieving information of the object in three dimensions. In FTH, the hologram is recorded as the interference between the object wave and a spherical reference wave, generated by a point source. Thus, the resolution is set by the size of the reference point source. The reference wave is typically created by a pinhole fabricated directly into an opaque screen located in the object's plane. This means the resolution is limited by the fabrication techniques currently available to create a small pinhole aperture. In contrast, CDI doesn't utilize any optics. As a result, the resolution in CDI is not restricted by fabrication techniques. However, CDI, which utilizes IPR can be sensitive to noise, has complicated data analysis, and consequently long reconstruction times. The IPR technique can potentially have non-unique solutions and difficulties with optically thick samples or samples with a variable transmission, complicating its use in *e.g.*, three-dimensional tomography [8]. Both techniques have been utilized for high-resolution imaging, tomography [9–12] and femtosecond imaging [13, 14]. In 2007, a generalization to FTH was developed utilizing extended references instead of point source references [15, 16] in what was defined as "holography with extended reference by autocorrelation linear differential operation" (HERALDO). This technique uses generalized reference sources to increase the reference-to-object signal ratio and improve the reconstruction quality. However, the reconstruction process requires the use of the directional derivative that can make it sensitive to noise.

In order to achieve simultaneous high temporal and spatial resolutions and a fast unambiguous reconstruction process we opted for a FTH scheme utilizing a EUV tabletop laser. The experiment described in this paper utilizes a Fresnel zone plate to split the illumination beam into a reference and an object's wave, allowing for the generation of a large intensity reference source, ultimately permitting large objects to be imaged [17]. The short-pulsed illumination (~1.2 ns) enables simultaneously time-resolved (or "flash") holography with the capability to acquire images of nanoscale objects oscillating at MHz frequencies. Additionally the setup described in this work, utilizes a tabletop EUV laser source with a large coherent photon flux. The compact EUV laser allows for both high spatial and temporal resolutions for the holographic recording in a tabletop system. The fast and simple reconstruction algorithm requires very modest computational requirements to obtain images of sub-micron fast moving objects and enables an almost "live" visualization of the object.

2. Time-resolved Fourier transform holography

The scheme of the experimental setup is depicted in Fig. 1. It is capable of recording 1.2 ns temporal and 128 nm spatial resolution holograms [18]. A zone plate optic was used as a beam splitter to generate the illumination (object) beam and the reference point source. The zone plate utilized in this experiment has a diameter of 0.5 mm and an outermost zone width (Δr) of 100 nm. At the laser wavelength, its focal length is 1.1 mm and the corresponding numerical aperture is 0.23, with ± 430 nm depth of focus. The incident beam impinges on the zone plate and then splits into multiple orders. The first order focus was used to produce a point source that generates the reference wave and a 50 μm central opening in the zone plate allowed the incident beam to directly illuminate the object with an almost plane wavefront (Fig. 1). The other orders were filtered out by a small pinhole made in the object's mask.

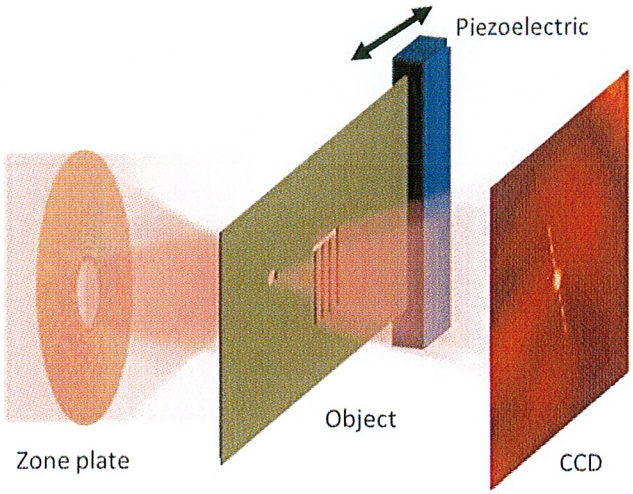

Fig. 1. The beam is incident on the zone plate from the left. The central opening in the zone plate passed the incident beam directly to illuminate the object while the 1st order focus was used as the reference wave. The interference between the two beams was collected on a CCD and numerically reconstructed to obtain the final image.

The mask consists of a window (~15 × 4 μm^2) where the object was fabricated. The object was composed of three pillars fabricated by focused ion beam in a 200 nm thick Si_3N_4 membrane with a 200 nm gold coating. The gold coating was deposited to block the broadband plasma emission from the EUV laser and constrain the signal after the object plane to the diffracted wave in the object and the reference point source. This effectively increases the signal-to-noise ratio and allows for single-shot exposures. The pillars moved due to an excitation produced by a piezo-electric actuator driven by a sinusoidal voltage signal at a frequency of ~1MHz. The motion of the pillars is clearly detected in the holograms recorded as deflections in the pillar from the rest positions. The small pinhole is located at a proper distance to satisfy separation conditions for FTH [19], in this case 16.7 μm from the center of the object. The interference between the object and reference waves is collected on an X-ray Peltier cooled CCD camera with a 26.7 × 26.7 mm^2 CCD chip, having 13.5 μm wide square pixels and a total array size of 2048 × 2048 pixels. The CCD detector was located at a distance of 5.4 cm from the object plane.

The laser source used in this holographic system is a compact EUV laser emitting a highly coherent beam at λ = 46.9 nm. The main characteristics of the laser are its high energy per pulse (typically 0.2-0.5 mJ) [20], its compact size (a footprint 1 × 0.75 m^2), its small bandwidth ($\Delta\lambda/\lambda$ ~3-4 10^{-5}) [21] and its smooth beam intensity profile. The spatial coherence was calculated to be 750 μm at the zone plate position that assures a fully spatially coherent illumination. However, this is not a limiting factor if larger objects are sought to be imaged since the spatial coherence can be enhanced by increasing the length of the amplifier medium to produce a fully spatial coherent beam for 36 cm long capillaries [22].

3. Experimental setup and results

Figure 2 shows an SEM image of the sample (a), a hologram (b), and the corresponding reconstruction (c). The reconstruction is obtained by two-dimensional inverse FFT of the hologram shown in (b). The oscillating pillars are 250 nm wide and 15 μm long. Flash

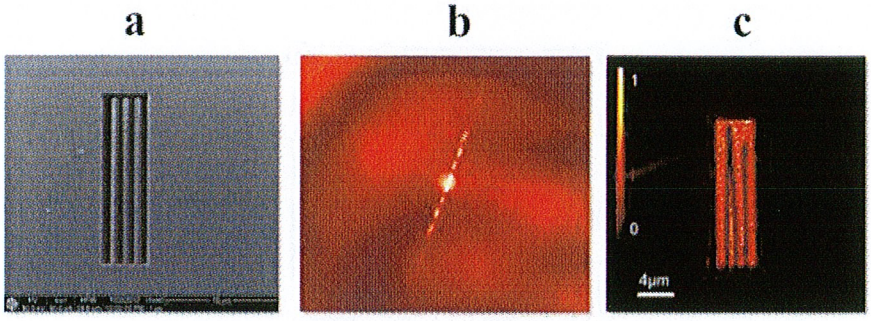

Fig. 2. (a) SEM of three nanopillars fabricated using a focused ion beam. (b) The central portion of the hologram taken with a single-shot EUV pulse. (c) The reconstruction of the pillars by reconstructing the hologram in (b). The pillar on the right appears shorter because it is deflected in the direction of the optical axis.

holograms (1.2 ns exposure time) were recorded to acquire images of the pillars while they were vibrating. The nanosecond acquisition time allows for "frozen" images of the oscillating nanopillars that otherwise would appear blurred along the direction of movement.

The displacement of the pillars is evident in the reconstructions shown in Fig. 3 which were acquired at different times during the periodic oscillation. The third pillar is clearly displaced from its rest position indicating that it is vibrating in the object's plane. Taking successive single-shot holograms of the oscillating pillars it is possible to compose a sequence which clearly shows the movement. The sequence of images featuring a movie of vibrating pillars can be accessed in Media 1.

The single-shot holograms were transformed into grey-scaled images that were imported into a data analysis program where the location of the intensity maximum for each row of pixels and for each pillar can be found to the sub-pixel accuracy. Then, each pillar shape is fitted to a corresponding shape of a vibrating cantilever beam, based on the shape of the first resonance for an Euler beam. Figure 4 shows the results of the analysis performed on 6 holograms, a sub-set of images that composes the movie shown in the supplementary files. The best fits to the images are shown in red lines in Fig. 4. The agreement between theory and experiment is excellent and thus shows that Euler beam with uniform (but orientation-dependent) properties is an adequate model for describing the vibrating pillars, even for large displacements from the resting position like the fits shown in the last two rightmost images. Reconstruction of the holograms allows also for retrieval of information on the position of the pillars in the longitudinal axis (along the beam propagation) as well. The rightmost pillar in

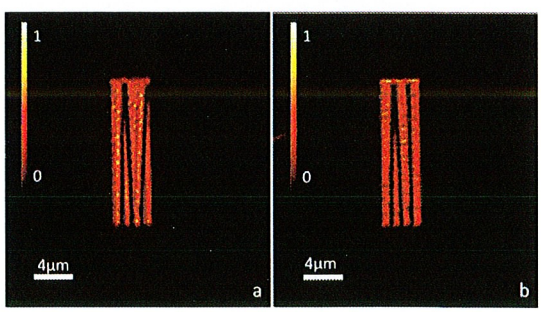

Fig. 3. Two reconstructions of the pillars in different positions as the pillar on the right vibrates due to the piezoelectric driving force. A sequence of holograms featuring a movie of the oscillation of the pillars can be found in Media 1.

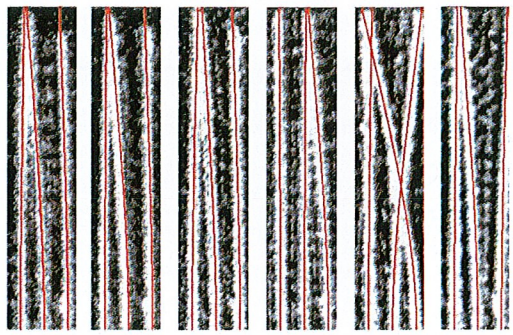

Fig. 4. Example of the analysis of an image of oscillating pillars. The red lines are the best fits corresponding to a vibrating cantilever based on the shape of the first resonance for Euler beam.

Figure 2(c) appears to be shorter than the others. This is due to the fact that it is bent out of plane in the direction of the optical axis. To retrieve the depth information we utilized Fresnel back-propagation and analyzed the images obtained by reconstructing the hologram shown in Fig. 2(b) at different depths (z-values). In each reconstruction we determined the region of the image along the pillar that is in focus, *i.e.*, finding the position along the pillar where the resolution of the image is maximum using the knife-edge test. Figure 5 shows three reconstructions at different depths along the optical axis, obtained from the hologram shown in Fig. 2(b). The reconstruction distances were $z = -2\mu m$, $z = -5\mu m$ and $z = -10\mu m$, and were measured from the plane where the point reference source is located. The knife edge analysis indicated that the bottom, middle and top sections of the pillar are in focus for Figs. 5(a), 5(b) and 5(c), respectively. This effect is represented schematically in the illustrations on the right showing the relative focus-plane positions as it intersects the bent pillar. From these reconstructions a 3D profile can be calculated which is instrumental for determining the time-resolved pillar dynamics. Along the propagation axis the resolution is limited to the depth of focus of the zone plate which in our experiment is ± 430 nm. Thus, with this series of reconstructions from a single hologram it was possible to determine that the tip of the pillar was deflected by $\Delta z = (8 \pm 0.43)\ \mu m$ relative to the bottom section of the pillar.

4. Discussion

Using the experimental technique outlined here it is possible to map the time-resolved hologram to the three-dimensional shape of the pillar. Since at all times, the pillar shape in each direction can be described with high accuracy by the first Euler beam resonant shape, any three-dimensional pillar shape observed in our experiment, can be approximated, to a high accuracy, by a single two-dimensional vector describing the components of amplitude of deflection in the directions transversal and parallel to the axis. This is precisely the input that is needed for accurate comparison to the two-dimensional model developed in [23, 24]. It was shown that under the right condition, the system is captured in highly nonlinear, localized, periodic states called Intrinsic Localized Modes (ILMs). The good agreement with the model shown in the results depicted in Fig. 4 validates using the two dimensional vector model to describe the nonlinear theory of interacting pillar arrays [25]. This opens the possibility to apply this formalism to describe the appearance of ILMs in nanoscale mechanical oscillators.

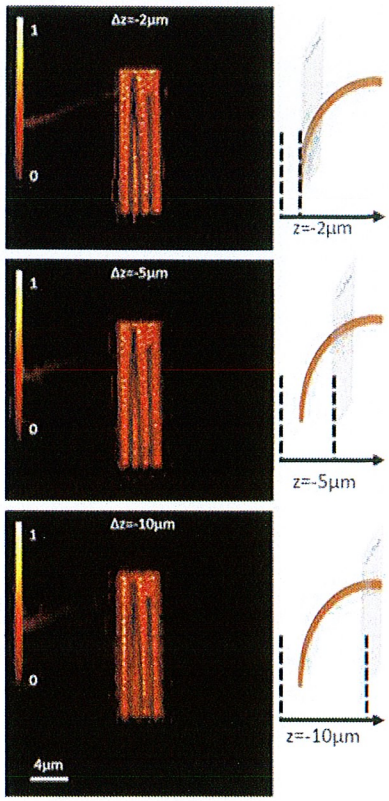

Fig. 5. The left column shows three reconstructions at three different depths (−2,-5 and −10μm) using a single hologram. The bottom and top sections appear in focus at z = −2 μm and z = −10 μm respectively. The right column shows a diagram of the rightmost pillar structure along the optical axis. The plane in the right column indicates the reconstruction plane in relation to the pillar.

5. Conclusion

In conclusion, single-shot EUV Fourier transform holography was implemented for the purpose of determining the nanoscale dynamics of fast moving objects, which in this case, are oscillating pillars. The 1.2 ns duration of the pulsed laser illumination allowed for "flash" holograms. The ability to refocus the reconstructions in Fourier transform holography allowed for the 3D pillar displacement to be determined from a single hologram. Our goal for the future is to observe the real-time motion of ILMs which has not been achieved in these scales [26]. A more far-reaching goal of this research is to use ILMs to detect foreign objects altering pillar dynamics with applications in sensing, with this paper forming one of the first essential steps of this objective [23].

Acknowledgments

The authors acknowledge support by the Defense Threat Reduction Agency – Joint Science and Technology office for Chemical Biological Defense (Grant No. HDTRA1-10-1-007) and the National Science Foundation Engineering Research Center for Extreme Ultraviolet Science and Technology award EEC 0310717.

This work was supported by the Director, Office of Science, of the U.S. Department of Energy under Contract No. DE-AC02-05CH11231.